

Graphical Abstract

A Linear Quadratic Integral Differential Game Approach for Attitude Control of an Experimental Platform of a Quadrotor

Hadi Nobahari, Ali BaniAsad, Reza Pordal, Alireza Sharifi

A Linear Quadratic Integral Differential Game Approach for Attitude Control of an Experimental Platform of a Quadrotor

Hadi Nobahari, Ali BaniAsad, Reza Pordal, Alireza Sharifi

^a*Department of Aerospace Engineering Sharif University of Technology, Tehran, Iran*

Abstract

This research paper presents a novel approach to quadrotor attitude control that draws on differential game theory. The approach uses a linear quadratic Gaussian (LQG) controller with integral actions. Accurate attitude control is of utmost importance for safe and effective quadrotor flight, particularly in the presence of disturbances. To develop a dependable and effective control system, the motion equations with nonlinearity for the quadrotor's experimental setup are transformed into a continuous-time state-space model through linearization. Experimental data are used to identify model parameters, and attitude control commands are determined using two-player approaches. By mini-maximizing a quadratic set of criteria, which is the total of the outputs and disturbances weighted by the amount of control effort, one player minimizes the command while the other generates disturbances. The performance of the proposed approach is evaluated by comparing it to a linear quadratic regulator controller in level flight. The results demonstrate that the proposed approach effectively dissipates disturbances and outperforms linear quadratic regulator controllers, thereby contributing to the development of robust and effective attitude control systems for quadrotors.

Keywords:

Linear quadratic Gaussian controller, Differential game theory, Quadrotor, Continuous state-space model, three-degree-of-freedom experimental platform, Attitude Control Optimization, Robust disturbance rejection.

Email addresses: nobahari@sharif.edu (Hadi Nobahari),
ali.baniasad@ae.sharif.edu (Ali BaniAsad), email address (Reza Pordal),
alireza_sharifi@ae.sharif.edu (Alireza Sharifi)

1. Introduction

The investigation, strategic operations, optical sensing, entertainment, and farming are all used by quadrotors in today's society (Fathoni et al., 2021).

2. Problem Formulation

The experimental quadrotor platform rotates freely with rotational velocity about its roll, pitch, and yaw axes, as shown in Figure 1. The Euler angles and their derivatives are measured using an Attitude Heading Reference System (AHRS), which is utilized in the structure of the LQIR-DG controller to stabilize the quadrotor platform. The graphical representation of the proposed controller structure is depicted in Figure 2.



Figure 1: 3DoF setup of the quadrotor.

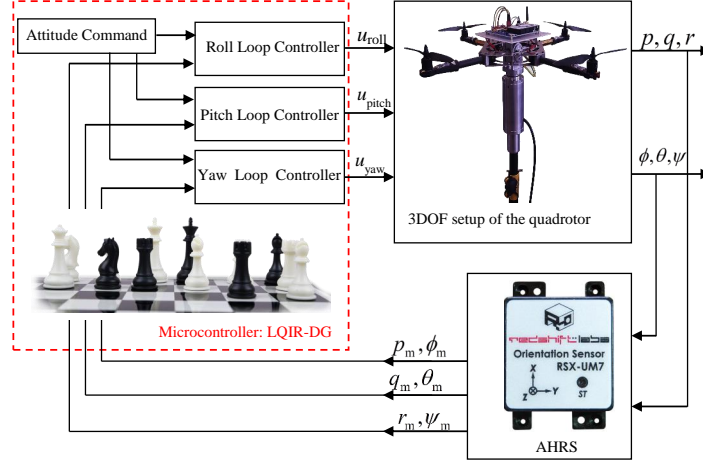


Figure 2: Structure of the LQIG-DG Controller Illustrated in a Block Diagram.

3. Dynamic Model of the Quadrotor Platform

In this section, first, a nonlinear model for the quadrotor platform is derived. Then, a state-space model and a linear model are developed for control purposes to be utilized in a controller strategy. Finally, a nonlinear identification method is applied to identify the parameters of the quadrotor.

3.1. Quadrotor Configuration

Figure 3 shows the quadrotor schematic. It depicts four rotors rotating around the z_B axis in the coordinate system of the body. The rotors have a rotational velocity of Ω_r . The quadrotor platform has 3 degrees of freedom, including roll, pitch, and yaw motions, which are described by roll (ϕ), pitch (θ), and yaw (ψ) angles, respectively. The counterclockwise rotation of Rotors 1 and 3 generates a moment that counteracts the yawing moment, while the clockwise rotation of Rotors 2 and 4 produces a moment that also counteracts the yawing moment.

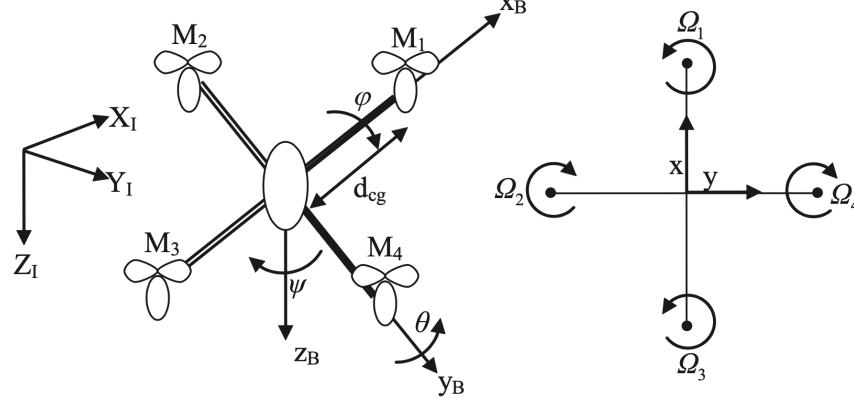


Figure 3: Quadrotor Configuration.

3.2. Dynamic Modeling of the Quadrotor Platform

Here, according to Newton-Euler, the dynamic model of the quadrotor platform is derived as follows Bouabdallah and Siegwart (2007); Bouabdallah (2007):

$$\dot{p} = \frac{I_{yy} - I_{zz}}{I_{xx}}qr + q\frac{I_{\text{rotor}}}{I_{xx}}\Omega_r + \frac{u_{\text{roll}}}{I_{xx}} + \frac{d_{\text{roll}}}{I_{xx}} \quad (1)$$

$$\dot{q} = \frac{I_{zz} - I_{xx}}{I_{yy}}rp + p\frac{I_{\text{rotor}}}{I_{xx}}\Omega_r + \frac{u_{\text{pitch}}}{I_{yy}} + \frac{d_{\text{pitch}}}{I_{yy}} \quad (2)$$

$$\dot{r} = \frac{I_{xx} - I_{yy}}{I_{zz}}pq + \frac{u_{\text{yaw}}}{I_{zz}} + \frac{d_{\text{yaw}}}{I_{zz}} \quad (3)$$

The (p, q, r) represent the rotational variables, and d_{roll} , d_{pitch} , and d_{yaw} denote the disturbances produced in the x_B , y_B , and z_B axes, respectively. Additionally, I_{xx} , I_{yy} , and I_{zz} are the principal moments of inertia, and I_{rotor} is the rotor inertia about its axis. Euler angle rates are also determined from angular body rates as follows:

$$\begin{bmatrix} \dot{\phi} \\ \dot{\theta} \\ \dot{\psi} \end{bmatrix} \begin{bmatrix} 1 & \sin(\phi)\tan(\theta) & \cos(\phi)\tan(\theta) \\ 0 & \cos(\phi) & -\sin(\phi) \\ 0 & \sin(\phi)/\cos(\theta) & \cos(\phi)/\cos(\theta) \end{bmatrix} \begin{bmatrix} p \\ q \\ r \end{bmatrix} \quad (4)$$

The residual rotor velocity, denoted by Ω_r , is calculated as follows:

$$\Omega_r = -\Omega_1 + \Omega_2 - \Omega_3 + \Omega_4 \quad (5)$$

3.3. Input of the Dynamic Model

The control inputs u_{roll} , u_{pitch} , and u_{yaw} are to the moments generated by the quadrotor's rotors along the roll, pitch, and yaw axes, respectively, defined as follows:

$$u_{\text{roll}} = b d_{\text{cg}} (\Omega_2^2 - \Omega_4^2) \quad (6)$$

$$u_{\text{pitch}} = b d_{\text{cg}} (\Omega_1^2 - \Omega_3^2) \quad (7)$$

$$u_{\text{yaw}} = d(\Omega_1^2 - \Omega_2^2 + \Omega_3^2 - \Omega_4^2) \quad (8)$$

where d_{cg} , d , and b represent the distance between the rotors and the gravity center, drag factor, and thrust factor, respectively. The rotational velocity commands are computed as follows:

$$\Omega_{c,1}^2 = \Omega_{\text{mean}}^2 + \frac{1}{2b d_{\text{cg}}} u_{\text{pitch}} + \frac{1}{4d} u_{\text{yaw}} \quad (9)$$

$$\Omega_{c,2}^2 = \Omega_{\text{mean}}^2 + \frac{1}{2b d_{\text{cg}}} u_{\text{roll}} - \frac{1}{4d} u_{\text{yaw}} \quad (10)$$

$$\Omega_{c,3}^2 = \Omega_{\text{mean}}^2 - \frac{1}{2b d_{\text{cg}}} u_{\text{pitch}} + \frac{1}{4d} u_{\text{yaw}} \quad (11)$$

$$\Omega_{c,4}^2 = \Omega_{\text{mean}}^2 - \frac{1}{2b d_{\text{cg}}} u_{\text{roll}} - \frac{1}{4d} u_{\text{yaw}} \quad (12)$$

In the above equation, Ω_{mean} is nominal rotational velocities of the rotors.

3.4. State-Space Formulation

Here, by defining $x_1 = p$, $x_2 = q$, $x_3 = r$, $x_4 = \phi$, $x_5 = \theta$, and $x_6 = \psi$, the formulation of the quadrotor platform is presented as follows:

$$\dot{x}_1 = \Gamma_1 x_2 x_3 + \Gamma_2 x_2 \Omega_r + \Gamma_3 u_{\text{roll}} + \Gamma_3 d_{\text{roll}} \quad (13)$$

$$\dot{x}_2 = \Gamma_4 x_1 x_3 - \Gamma_5 x_1 \Omega_r + \Gamma_6 u_{\text{pitch}} + \Gamma_6 d_{\text{pitch}} \quad (14)$$

$$\dot{x}_3 = \Gamma_7 x_1 x_2 + \Gamma_8 u_{\text{yaw}} + \Gamma_8 d_{\text{yaw}} \quad (15)$$

$$\dot{x}_4 = x_1 + (x_2 \sin(x_4) + x_3 \cos(x_4)) \tan(x_5) \quad (16)$$

$$\dot{x}_5 = x_2 \cos(x_4) - x_3 \sin(x_4) \quad (17)$$

$$\dot{x}_6 = (x_2 \sin(x_4) + x_3 \cos(x_4)) / \cos(x_5) \quad (18)$$

where $\Gamma_i (i = 1, \dots, 8)$ is defined as:

$$\begin{aligned}\Gamma_1 &= \frac{I_{yy} - I_{zz}}{I_{xx}}, & \Gamma_2 &= \frac{I_{\text{rotor}}}{I_{xx}}, & \Gamma_3 &= \frac{1}{I_{xx}} \\ \Gamma_4 &= \frac{I_{zz} - I_{xx}}{I_{yy}}, & \Gamma_5 &= \frac{I_{\text{rotor}}}{I_{xx}}, & \Gamma_6 &= \frac{1}{I_{yy}} \\ \Gamma_7 &= \frac{I_{xx} - I_{yy}}{I_{zz}}, & \Gamma_8 &= \frac{1}{I_{zz}}\end{aligned}\quad (19)$$

Moreover, the measurement vector, obtained from the AHRS sensor is presented as follows:

$$\mathbf{z} = [p \ q \ r \ \phi \ \theta \ \psi]^T + \boldsymbol{\nu} \quad (20)$$

where $\boldsymbol{\nu}$ is a Gaussian white noise. In the above equation, the superscripts T indicate the transpose notation.

3.5. Linear Model

The linear continuous-time model of the quadrotor platform about the equilibrium points ($\mathbf{x}_e = \mathbf{0}$ and $\mathbf{u}_e = \mathbf{0}$) is represented as:

$$\dot{\mathbf{x}}(t) = \mathbf{A} \mathbf{x}(t) + \mathbf{B} \mathbf{u}(t) + \mathbf{B}_d \mathbf{d}(t) \quad (21)$$

where $\dot{\mathbf{x}} = [\dot{\mathbf{x}}_{\text{roll}} \ \dot{\mathbf{x}}_{\text{pitch}} \ \dot{\mathbf{x}}_{\text{yaw}}]$, defined as:

$$\mathbf{x}_{\text{roll}} = \begin{bmatrix} p \\ \phi \end{bmatrix}, \quad \mathbf{x}_{\text{pitch}} = \begin{bmatrix} q \\ \theta \end{bmatrix}, \quad \mathbf{x}_{\text{yaw}} = \begin{bmatrix} r \\ \psi \end{bmatrix} \quad (22)$$

Moreover, \mathbf{B} and \mathbf{B}_d are the input and disturbance matrices, respectively, and are defined as:

$$\mathbf{B} = \mathbf{B}_d = \begin{bmatrix} \mathbf{B}_{\text{roll}} & \mathbf{0} & \mathbf{0} \\ \mathbf{0} & \mathbf{B}_{\text{pitch}} & \mathbf{0} \\ \mathbf{0} & \mathbf{0} & \mathbf{B}_{\text{yaw}} \end{bmatrix} \quad (23)$$

In addition, the input matrices and state are shown as:

$$\mathbf{A}_{\text{roll}} = \mathbf{A}_{\text{pitch}} = \mathbf{A}_{\text{yaw}} = \begin{bmatrix} 0 & 0 \\ 1 & 0 \end{bmatrix} \quad (24)$$

$$\mathbf{B}_{\text{roll}} = \begin{bmatrix} \frac{1}{I_{xx}} \\ 0 \end{bmatrix}; \quad \mathbf{B}_{\text{pitch}} = \begin{bmatrix} \frac{1}{I_{yy}} \\ 0 \end{bmatrix}; \quad \mathbf{B}_{\text{yaw}} = \begin{bmatrix} \frac{1}{I_{zz}} \\ 0 \end{bmatrix} \quad (25)$$

3.6. Identification of the Platform Parameters

This section describes the utilization of the Nonlinear Least Squares (NLS) algorithm for estimating the model parameters (Γ) of the 3DoF experimental platform using experimental data. This technique is based on the Trust-Region Reflective Least Squares (TRRLS) method, which iteratively finds the values of the model parameters by minimizing a cost function, defined as follows:

$$\min_{\Gamma_i} (\| e(\Gamma_i) \|^2) = \min_{\Gamma_i} = \left(\sum_{j=1}^n (z_j - \hat{z}_j)(z_j - \hat{z}_j)^T \right) \quad (26)$$

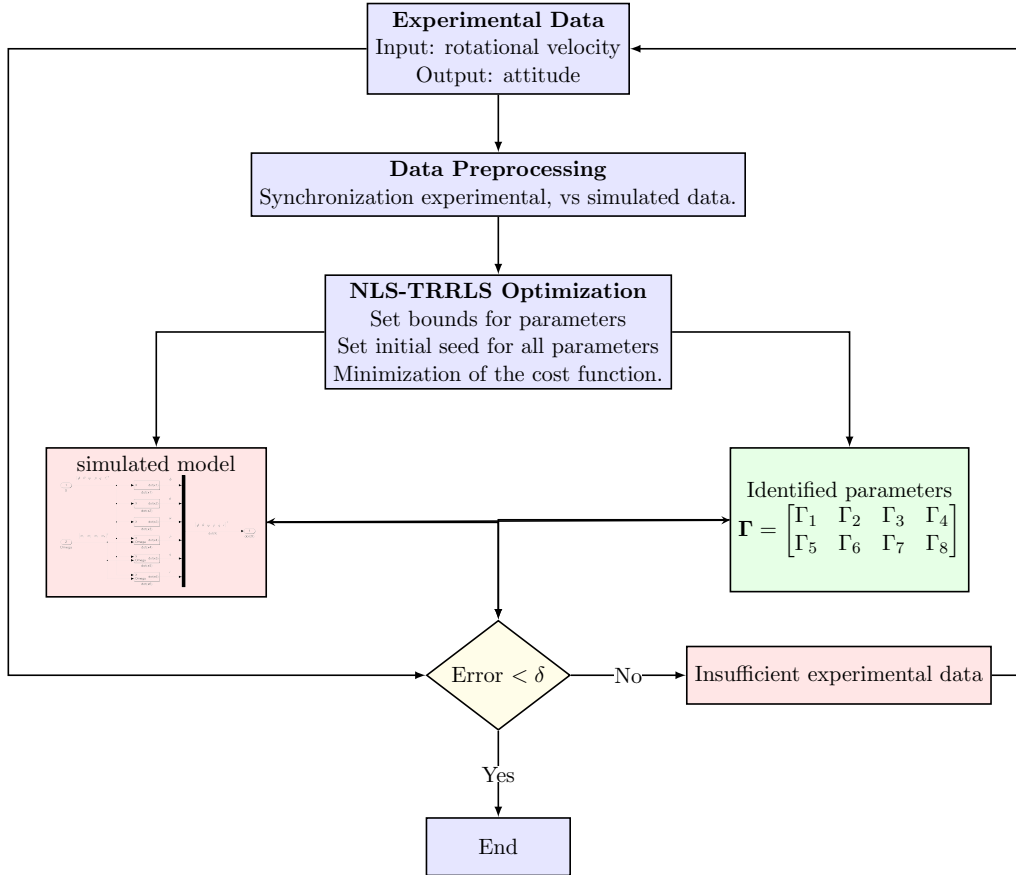


Figure 4: Structure of TRRLS identification approach.

References

- Bouabdallah, S., 2007. Design and control of quadrotors with application to autonomous flying doi:10.5075/epfl-thesis-3727.
- Bouabdallah, S., Siegwart, R., 2007. Full control of a quadrotor, in: 2007 IEEE/RSJ International Conference on Intelligent Robots and Systems, pp. 153–158. doi:10.1109/IROS.2007.4399042.
- Fathoni, M.F., Lee, S., Kim, Y., Kim, K.I., Kim, K.H., 2021. Development of multi-quadrotor simulator based on real-time hypervisor systems. Drones 5. URL: <https://www.mdpi.com/2504-446X/5/3/59>, doi:10.3390/drones5030059.